ELSEVIER

Journal of Biomechanics 34 (2001) 1661–1665

JOURNAL OF BIOMECHANICS

www.elsevier.com/locate/jbiomech
www.JBiomech.com

Technical note

In vivo biomechanical behavior of the human heel pad during the stance phase of gait

Amit Gefen[a,*], Michal Megido-Ravid[b], Yacov Itzchak[b]

[a] *Department of Biomedical Engineering, Faculty of Engineering, Tel Aviv University, Tel Aviv 69978, Israel*
[b] *Department of Diagnostic Imaging, The H. Sheba Medical Center, Tel Hashomer 52621, Israel*

Accepted 3 July 2001

Abstract

A technique is introduced for simultaneous measurements of the heel pad tissue deformation and the heel–ground contact stresses developing during the stance phase of gait. Subjects walked upon a gait platform integrating the contact pressure display optical method for plantar pressure measurements and a digital radiographic fluoroscopy system for skeletal and soft tissue motion recording. Clear images of the posterior-plantar aspect of the calcaneus and enveloping soft tissues were obtained simultaneously with the pressure distribution under the heel region throughout the stance phase of gait. The heel pad was shown to undergo a rapid compression during initial contact and heel strike, reaching a strain of 0.39 ± 0.05 in about 150 ms. The stress–strain relation of the heel pad was shown to be highly non-linear, with a compression modulus of 105 ± 11 kPa initially and 306 ± 16 kPa at 30% strain. The energy dissipation during heel strike was evaluated to be $17.8 \pm 0.8\%$. The present technique is useful for biomechanical as well as clinical evaluation of the stress–strain and energy absorption characteristics of the heel pad in vivo, during natural gait.

Keywords: Foot–ground contact stress; Walking; Radiographic fluoroscopy; Plantar pressure; Soft tissue mechanical properties

1. Introduction

The impacting stress waves acting on the foot during walking must be reduced during each stance phase of the gait cycle to minimize their transfer to the skeletal system. In order to absorb the impact energy, the foot that contacts the ground undergoes substantial joint and tissue deformation. The fat pad under the heel, with an average thickness of 18 mm in the adult male, plays an important role in protecting the underlying bones. It is comprised of sealed spiral microchambers of unsaturated fat contained in whorls of fibroelastic tissue, which is anchored to both the dermis (skin) and the calcaneus (Jorgensen, 1985).

Evaluations of the response of the heel pad to impact were conducted in loading conditions that simulated the heel strike stage of walking, e.g. by utilizing pendulums or motorized cams to induce impacts on heels of lying subjects, or through human drop tests (Jorgensen and Ekstrand, 1988; Aerts et al., 1995). The in vitro response of cadaveric heel pad specimens to impacting and cyclic loads generated by Instron testing machines was also evaluated (Jorgensen and Bojsen-Moller, 1989; Bennett and Ker, 1990). Although these in vivo and in vitro studies provided some quantitative evaluations of the resiliency of the heel pad and its energy absorbing properties, the use of mechanically simulated impacts is limiting their application for evaluating the heel pad functionality during actual gait. In later studies, De Clercq et al. (1994) characterized the in vivo deformation of the heel pad during barefoot and shod running using cineradiography while Cavanagh (1999) described a method for measuring the deformation of the plantar tissue using ultrasound imaging. However, these methods lack the ability to correlate the heel pad deformation during ground contact with the simultaneous heel–ground contact stress. The present paper describes a technique that allows for simultaneous measurements of the heel pad strain and the contact stresses developing under it during actual gait, for analysis of its functional role in attenuating the ground reactions.

*Corresponding author. Tel.: +972-3-640-8093; fax: +972-3-640-7939.
E-mail address: gefen@eng.tau.ac.il (A. Gefen).

0021-9290/01/$ - see front matter
PII: S0021-9290(01)00143-9

2. Methods

In the present study, two measurement methods were integrated to simultaneously record the deformation of the heel pad and the contact stresses developing during its interaction with the ground. A digital radiographic fluoroscopy (DRF) imaging system was used to measure the transient thickness of the heel pad while dynamic foot–ground contact pressure display (CPD) measurements provided the evolution of plantar pressures under the foot (Fig. 1).

The DRF is a computerized X-ray-based clinical examination system that displays and electronically records skeletal and soft tissue motion and thus, could be utilized to observe the deformation of the heel pad during gait (Fig. 2(a)). The Philips Multi Diagnost 3 (MD3) DRF system was used for the experiments. The CPD is an optical method for measuring the foot–ground pressure by means of a birefringent optical sandwich (see Gefen et al., 2000 for a review). The CPD method was selected because of its versatility, which allowed for construction of a pressure-sensitive area in dimensions that could be easily fitted into the DRF system. Digital image sampling of the CPD images (Fig. 2(c)) was carried out using a $\frac{1}{2}''$ CCD video camera with 600 TV lines (Chiper, CPT-8360).

A DRF/CPD gait platform of 2.5 m length was mounted on the MD3 examination table (Fig. 1). Subjects walked while being hand-supported for a safer feeling and dynamic body balance. This was considered during the measurement process by training subjects prior to data acquisition to avoid, as much as possible, transferring weight to the rails of the gait platform. Using a digital video capture board (Miro 20TD), the initial sampling rate of DRF/CPD frames was determined as 80 Hz, and following omission of distorted

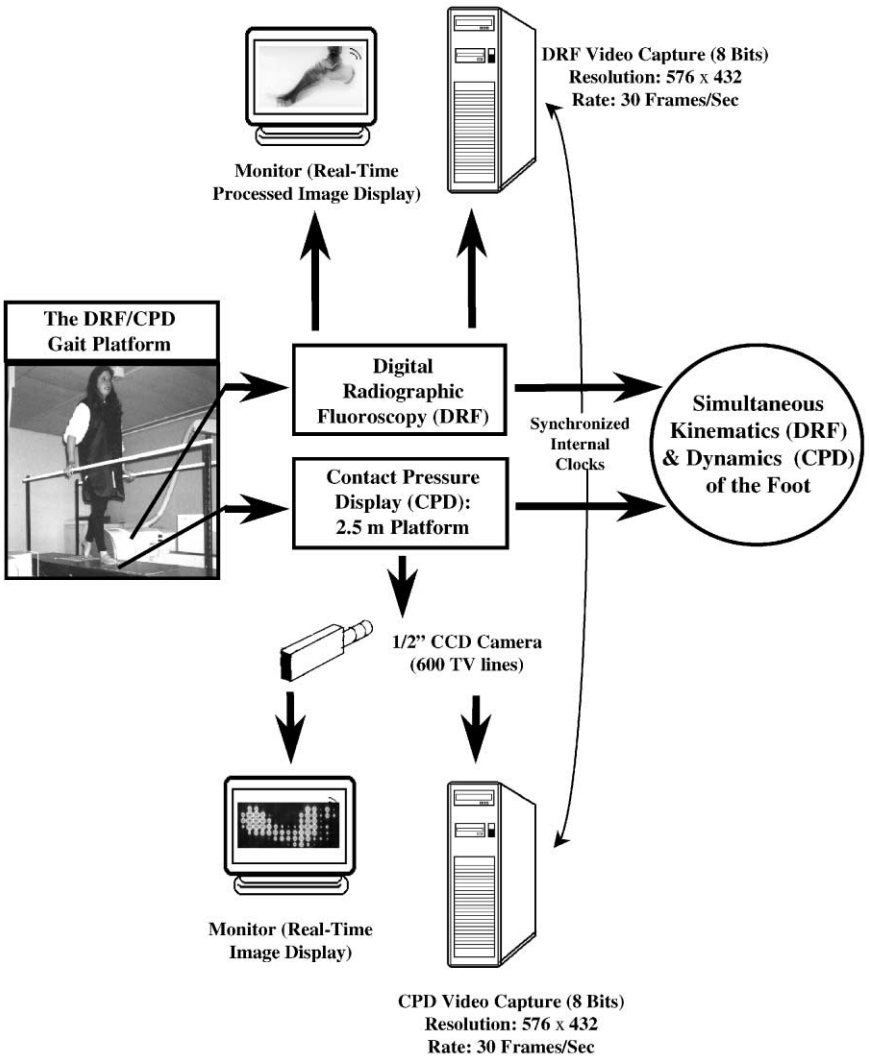

Fig. 1. Simultaneous acquisition of skeletal/soft tissue motion and plantar pressures during the stance phase of gait: schematic description of the DRF/CPD experimental setup.

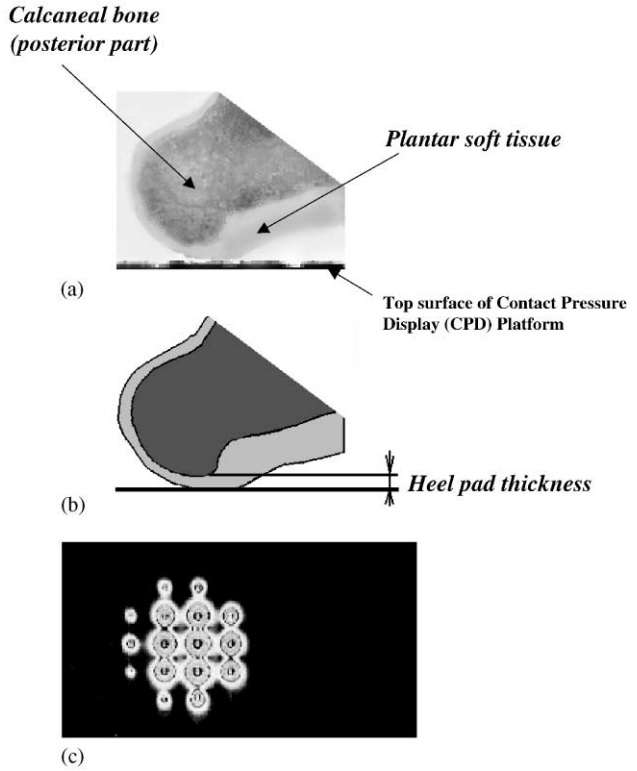

Fig. 2. Determination of the heel pad deformation due to the ground impact: (a) a representative radiographic image of the posterior aspect of the calcaneal bone and enveloping soft tissue during midstance, (b) segmentation of hard/soft tissue and contour detection allowing digital measurement of the transient heel pad thickness, and (c) the contact pressure display (CPD) visualization of the corresponding distribution of heel–ground contact stresses for this position of the heel.

frames, a set of up to 30 high-quality frames per second with a resolution of 576×432 pixels was obtained for each test. Two female volunteers with similar body characteristics (age: 27 and 35 years, weight: 58 and 60 kg) were dressed with a lead apron to minimize exposure to X-ray radiation and limit it to the feet. Each subject carried out four trials of walking on the DRF/CPD gait platform. Gait velocity of subjects ranged between 0.5 to 0.9 m/s. The DRF/CPD data were analyzed using video and image processing software, to obtain the time-dependent deformation of the heel pad in respect to the heel–ground contact stress. Hence, DRF frames were processed using segmentation and edge-detecting algorithms applied to the posterior aspect of the foot image, to clearly distinguish between the calcaneal bone and the subcalcaneal soft tissue. The thickness of the heel pad was then digitally measured on each processed frame, between the skin of the plantar face of the heel and the base of the calcaneus (Fig 2). The unloaded thickness of the heel pad was measured both prior to initial contact and following push-off, to yield the reference value for calculating the tissue strain. An error of 0.2 mm in the unloaded thickness measurements was accounted for, due to the spatial resolution of the acquired digital images. Additional error of 0.5 mm was introduced in the thickness measurements of the loaded heel pad due to absorption of the X-ray beam by the upper surface of the gait platform.

The value of the absolute heel pad deformation was calculated for each DRF frame of the stance phase as the difference between the loaded and unloaded thickness values. The compressive strain of the heel pad, ε_c was calculated as the ratio of absolute deformation to unloaded thickness. The overall error in the heel pad strain measurements was evaluated as the square root of the sum of squares of the partial errors (caused by spatial resolution and X-ray absorption), and found to be 5% maximally. The heel–ground contact stress (σ_c) was calculated for each CPD frame by averaging the contact stresses measured in each optical sensor under the heel–ground contact region. The contact stress (σ_c) versus the heel pad compression strain (ε_c) values were fitted to the following viscoelastic constitutive law to describe the in vivo stress–strain behavior of the human heel pad during gait:

$$\sigma_c = -E\varepsilon_c - \eta\varepsilon_c\dot{\varepsilon}_c, \tag{1}$$

where $\dot{\varepsilon}_c$ is the strain rate and E, η are the elastic and viscous parameters of the tissue, respectively. The relation given in Eq. (1) details the mechanical behavior of a modified Voight–Kelvin model, containing a linearly elastic spring in parallel to a non-linear damper (Fig. 3). This model was shown to adequately represent the in vivo stress–strain characteristics of the heel pad, and could thereby be used to calculate its elastic and viscous constants, by means of curve fitting.

Energy absorption in the heel pad was derived from the in vivo stress–strain relations. A hysteresis loop was shown to exist in the stress–strain relations, bounded by

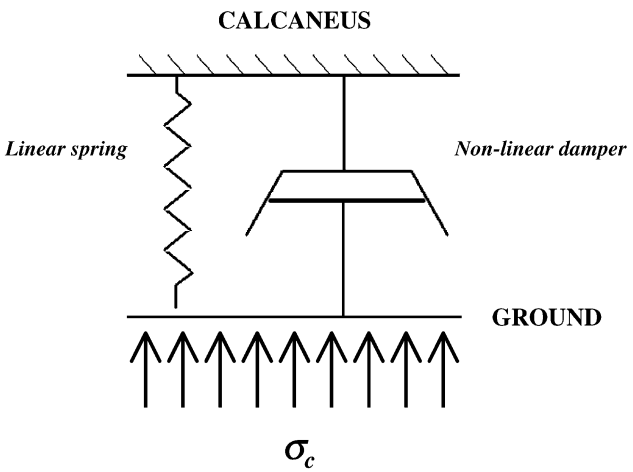

Fig. 3. Modified Kelvin–Voight viscoelastic model with a non-linear damper representing the stress–strain characteristics of the heel pad in vivo.

the loading and unloading curves. The appearance of hysteresis indicates dissipation of energy in the tissue. The energy attenuation of the heel pad, ξ^{h}, in terms of percentage of the total impact energy applied to the heel, was numerically calculated from the stress–strain data, by

$$\xi^{h} = \frac{\oint_{h} \sigma^{h}\, d\varepsilon}{\int_{0}^{\varepsilon_{max}} \sigma^{h}\, d\varepsilon}. \quad (2)$$

The numerator integral of Eq. (2) specifies the area bounded within the hysteresis loop, and indicates the energy absorbed due to the viscous properties of the tissue. The denominator integral specifies the area bounded between the loading curve and the horizontal axis, and indicates the energy applied to the heel by the ground impact.

3. Results

High-quality images of the calcaneal bone and subcalcaneal soft tissue were consistently obtained using the integrative DRF/CPD gait platform and digital recording system. Representative tissue strain versus time curves for complete stance phases, from initial contact to toe-off, are plotted in Fig. 4(a). The unloaded thickness and the maximal absolute deformation (calculated as the maximal difference between the loaded and unloaded thickness) of the heel pad were obtained for the two subjects and are specified in Table 1.

The strain of the heel pad, shown in Fig. 4(a), was calculated as the ratio of absolute deformation to unloaded thickness. It was shown that during heel strike, the heel pad is compressed very rapidly, to a maximum average strain of -0.39 ± 0.05 in about 150 ms. The strain rate during initial contact and heel strike (initial slopes of Fig. 4(a)) was shown to be maintained approximately constant, at an average value of $2.5\pm0.5\,s^{-1}$. Substantially slower compression of the heel pad continued for about additional 50 ms during early midstance, after which the unloading phase was initiated. Fig. 4(b) shows representative relations of the heel pad strain to the heel–ground contact stress. The plantar soft tissue demonstrated a highly non-linear stress–strain behavior in vivo. The initial compression modulus of the heel pad was measured to be 105 ± 11 kPa, while in a strain value of 30%, it reached 306 ± 16 kPa. The averaged experimental stress–strain data of the four stance phases obtained from each subject were fitted to the mathematical model of the heel pad given in Eq. (1). The best fit, according to the least squares method, was obtained for an elastic compression modulus $E=175$ kPa and a viscosity constant $\eta=22$ kPa s. By numerically solving Eq. (2) to calculate the averaged energy absorbency, the human heel pad was found to dissipate $17.8\pm0.8\%$ of the total energy during gait in the slow-to-moderate velocities.

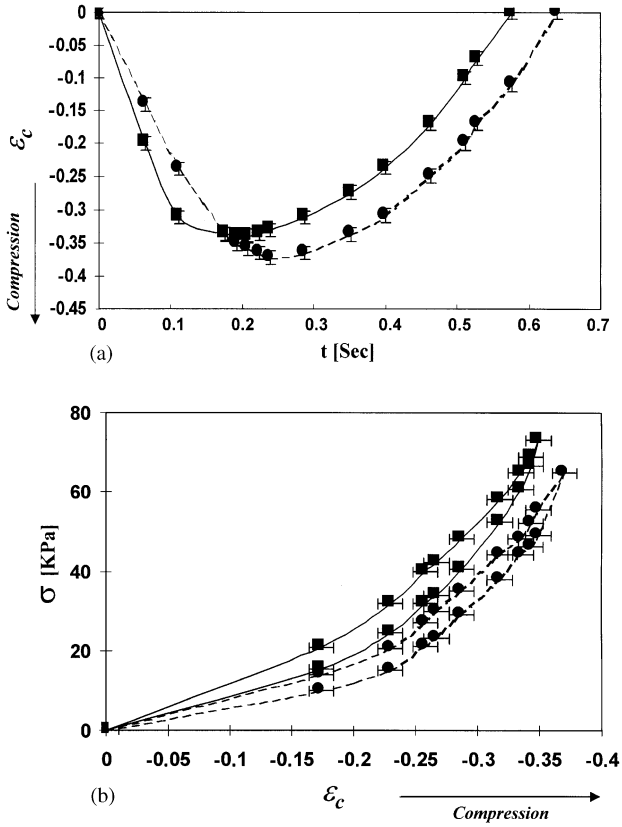

Fig. 4. Representative mechanical characteristics of the heel pad tissue in vivo during the stance phase of gait, obtained from two normal young subjects, marked as A (solid line) and B (dashed line): (a) the heel pad strain versus time and (b) the stress–strain relation. Negative strain values indicate compression.

Table 1
Body characteristics, unloaded thickness and maximal absolute deformation of the heel pad

		Subject A	Subject B
Age	(yr)	27	35
Weight	(kg)	58	60
Unloaded thickness	(mm)	11.2 ± 0.2	13.1 ± 0.2
Maximal deformation	(mm)	3.8 ± 0.5	4.8 ± 0.5

4. Discussion

An integrative DRF/CPD method for analysis of the mechanical characteristics of the heel pad in vivo, during the stance phase of gait, is described. The DRF/CPD method appears to be successful, repeatable, and applicable for the clinical setting, where it can be integrated into routine examinations of the foot and gait

performances. This method has a number of advantages as compared to previously suggested techniques. The optical pressure-sensitive plate can be easily mounted within a conventional clinical fluoroscopic imaging system, thus providing the contact stresses under the heel in addition to the vertical ground reactions provided by the setup of De Clercq (1994). In contrast to the ultrasound-based technique suggested by Cavanagh (1999) requiring full contact of the ultrasound probe with the soft tissue in order to measure its thickness, the present system provide measurements of tissue deformation when only minimal contact is made, as well as before and after ground contact. This allows for characterization of the complete loading–unloading cycle. Yet, it should be mentioned that the one-dimensional approach of measuring the heel pad thickness using lateral X-ray projections put some limitations on the interpretation of the results, as the true nature of the heel pad deformation is three dimensional. The necessity to dress subjects with a lead apron, which loaded them during the tests with approximately 4 kg, further affected the measured stress–strain behavior. In addition, the structure of the clinical DRF system prevented construction of a longer gait platform, which would allow for measurements of the heel pad properties in higher gait velocities.

It was demonstrated that during the heel strike stage of barefoot walking, the heel pad is compressed very rapidly, to a deformation of about 40% (Fig. 4(a)). This compression is, as expected, lower than the 60–66% deformation reported to occur during barefoot running (De Clercq et al., 1994) but yet, it is a critical factor for energy absorption in the viscoelastic tissue. By decelerating the calcaneal bone over the resilience medium of the heel pad during foot placement, the heel–ground peak stresses can be reduced (De Clercq et al., 1994). In the present study, the energy absorbance capacities of the heel pad in vivo during gait were measured to range between 17% and 19%. This result resembles the absorbency values of 20–28% measured by Paul et al. (1978) in heel pads of living rabbits, using implanted force transducers. However, it is considerably lower than values of 30–46% obtained for simulated heel strikes using instrumented pendulum apparatuses or a servo-hydraulic (Instron) axial compression testing system (Aerts et al., 1995; Ker, 1996; Pain and Challis, 2001). These discrepancies between measurements of the heel pad's energy absorption during real versus simulated gait should be further resolved through additional data collection.

References

Aerts, P., Ker, R.F., De Clercq, D., Ilsley, D.W., McNeil, A.R., 1995. The mechanical properties of the human heel pad: a paradox resolved. Journal of Biomechanics 28, 1299–1308.

Bennett, M.B., Ker, R.F., 1990. The mechanical properties of the human subcalcaneal fat pad in compression. Journal of Anatomy 171, 131–138.

Cavanagh, P.R., 1999. Plantar soft tissue thickness during ground contact in walking. Journal of Biomechanics 32, 623–628.

De Clercq, D., Aerts, P., Kunnen, M., 1994. The mechanical behavior characteristics of the human heel pad during foot strike in running: an in vivo cineradiographic study. Journal of Biomechanics 27, 1213–1222.

Gefen, A., Megido-Ravid, M., Itzchak, Y., Arcan, M., 2000. Biomechanical analysis of the three-dimensional foot structure during gait—a basic tool for clinical applications. Journal of Biomechanical Engineering 122, 630–639.

Jorgensen, U., 1985. Achillodynia and loss of heel pad shock absorbency. American Journal of Sports Medicine 13, 128–132.

Jorgensen, U., Bojsen-Moller, F., 1989. Shock absorbency of factors in the shoe/heel interaction, with special focus on the role of the heel pad. Foot Ankle 9, 294–299.

Jorgensen, U., Ekstrand, J., 1988. The significance of heel pad confinement for shock absorption at heel strike. International Journal of Sports Medicine 9, 468–473.

Ker, R.F., 1996. The time-dependent mechanical properties of the human heel pad in the context of locomotion. Journal of Experimental Biology 199, 1501–1508.

Pain, M.T.G., Challis, J.H., 2001. The role of the heel pad and shank soft tissue during impacts: a further resolution of the paradox. Journal of Biomechanics 34, 327–333.

Paul, I.L., Munro, M.B., Abernethy, P.J., Simon, S.R., Radin, E.L., Rose, R.M., 1978. Musculo–skeletal shock absorption: relative contribution of bone and soft tissues at various frequencies. Journal of Biomechanics 11, 237–239.